Proceedings of 2008 ASME Summer Heat Transfer Conference
HT2008
August 10-14, 2008, Jacksonville, Florida USA

HT2008-56455

Investigation of Potential Benefits of Using Bricks of High Thermal Capacity and Conductivity in A Rotating Calcining Kiln

Zhao Lei and Ting Wang
Energy Conversion and Conservation Center
University of New Orleans
New Orleans, LA 70148-2220, USA

ABSTRACT

Petroleum coke is processed into calcined coke in a rotary kiln, where the temperature profiles of flue gas and coke bed are highly nonuniform due to different flow and combustion mechanisms. Motivated by saving energy costs, the effect of refractory brick's thermal properties on potential energy savings is investigated. This study focuses on investigating potential energy savings by replacing inner one third of existing bricks with higher thermal capacity (Cp) and/or higher thermal conductivity (k) bricks. This investigation is motivated by postulating that the bricks with higher thermal capacity can store more thermal energy during the period of contacting with the hot gas and release more heat to the cock bed when the bricks rotate to below and in contact with the coke bed. A rotational, transient marching conduction numerical simulation is conducted using the commercial software FLUENT. The impact of brick heat capacity and thermal conductivity on transporting thermal energy to the coke bed is analyzed. The results show: (a) Increasing the heat capacity of brick layer reduces brick temperature which helps increase the heat transfer between the hot gas and brick, in other words it does help brick store more heat from the hot gas, but, heat transfer between brick and coke is reduced, which is opposite to the original postulation. (b) Higher brick thermal conductivity decreases brick temperature thus increases heat transfer between hot gas and the brick layer. The heat transfer from brick to coke bed is also increased, but not significantly. (c) Usually a brick with a higher Cp value also has a higher k-value. Simulation of a brick layer with both four times higher Cp and k values actually show appreciable heat is transported from the brick to the coke bed for one rotation for both lower and higher Cp and k bricks. The difference is not significant.

INTRODUCTION

A rotary kiln is used to calcine petroleum coke, and the product, calcined coke, is an important industrial material used for manufacturing graphite electrode for aluminum smelting process [1]. Inside the kiln, the volatile matters (released from the green coke) are burned to provide the energy for calcination while extra energy (mostly from natural gas) is supplied to maintain the required temperature near the discharge end. Due to different flow and combustion mechanisms, the temperature distribution inside the kiln is highly non-uniform, including in both the flue gas field and the coke bed. As a result, the rotary kiln wall also inherits a non-uniform temperature distribution. Figure 1 illustrates the heat transfer inside the kiln [2].

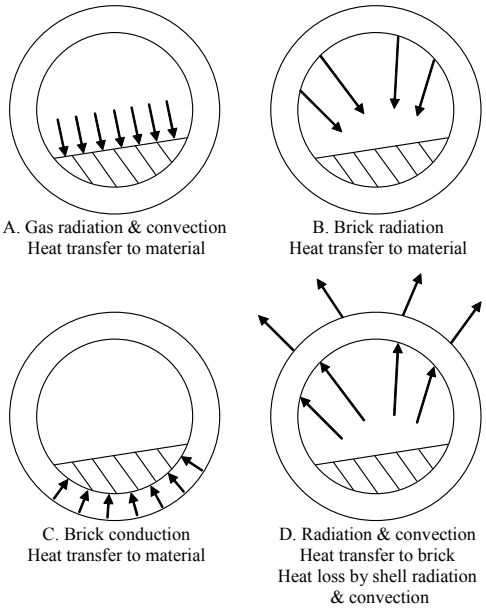

Figure 1 Modes of heat transfer in a rotary kiln [2]

Numerous experimental and numerical investigations on the thermal flow and transport phenomena inside the rotational kiln have been conducted and are available in the literature. Buir et al. [3] developed a mathematical model to simulate the calcination process of regular petroleum coke using 14 ordinary differential equations describing energy and mass conservation in the gas and in the coke bed with engineering correlations and algebraic equations. Dhanjal et al. [4] conducted an experimental study of heat transfer within the bed inside the rotary kiln by heating sand of varying particle-size distributions within a rotary kiln to bed temperatures up to 775 °C. The results suggested that segregation had little influence on heat transfer within the bed and that radial thermal gradients are primarily the result of inadequate particle mixing. Based on the insights of their experimental results, they developed a mathematical model for heat transfer within the transverse plane of the coke bed. Jochen et al. [5] developed a mathematical model for the range of rolling bed motion to calculate the transverse solids motion in rotating cylinders. They also conducted experiments and compared the results with both their calculation and those reported in literature. Gorog et al. [6] studied the radiative heat transfer between a nongray freeboard gas and the interior surfaces of a rotary kiln by evaluating the fundamental radiative exchange integrals using numerical methods.

Besides the heat transfer, the transport process of the rotary kiln has also been widely studied. John. et al. [7] studied the slow rotation of a cylindrical kiln which was partially filled with powder or granular solids. A penetration model was built that predicted the wall-to-bed heat transfer coefficients, leading to a better agreement with experiment when planar processes are omitted. Perron and Buir [8] proposed a semi-experimental model for predicting the axial transport of the granular bed in a rotating cylinder, based on dimensional and on the determination of an apparent viscosity characterizing the flow behavior of the bed. Henein et al. [9] developed a mathematical model to predict the conditions giving rise to the different forms of transverse bed motion in a rotary cylinder: slumping, rolling, slipping, cascading, cataracting, and centrifuging.

While previous studies have been focusing on the heat transfer and transport inside the kiln and bed, the heat transfer interactions between refractory brick layers and the hot gas and the coke bed have not been widely investigated. The heat transfer phenomenon is further complicated by the transient rotational motion of the kiln and stirring nature of the granular flow inside the bed. **Motivated** by the need to cutting the fuel cost by reducing natural gas consumption, the plausibility of employing different brick's thermal conductivities (k) and/or heat capacity (Cp) to achieve passive self-compensating effect of heat transfer from hotter to cooler regions is to be studied in this paper. It is **postulated** that with a higher heat capacity, the bricklayer may have a better ability to periodically absorb more heat from the hot gas, and then release more heat into the coke bed through the rotational process. To verify this postulation, the **objective** of this study is to develop a marching 2-D transient rotational scheme to simulate the 3-D brick wall situation and investigate the energy saving potential of using high heat capacity and/or high thermal conductivity bricks on the kiln wall.

MODELING AND METHODOLOGY

The studied problem involves different materials, heat convection, and thermal radiation inside the kiln as well as the effect of rotation. Numerical simulation is employed by using the commercial CFD software package, FLUENT (version 6.2.16), which has been qualified by many users in different studies and widely used by industry and academia.

Comparisons between different cases will be conducted focusing on heat transfer through the following interfaces: hot gas and coke bed (gas-bed) interface, hot gas and brick layer (gas-brick) interface, and brick layer and coke bed (brick-coke) interface.

Physical Configuration

The physical configuration of the studied kiln is shown in Fig. 2. The total length of the kiln is 60.96m (200 ft). The total thickness of the kiln refractory layer is 22.86 cm (9 inches) with a metal shell of 2.22 cm (7/8 inch) thick. The inner diameter of the kiln is 22.86 cm (9 feet). The maximum thickness of the coke bed is approximately 45.72 cm (1.5 feet). The coke bed occupies a sector of the circular cross-section with an included angle of approximately 96^o. While the coke bed in the real kiln consists of a dynamic granular flow with varying height and properties along the kiln, in this study, the height of the coke bed is assumed to maintain unchanged at 22.86 cm (9 inches). The rotation speed is assumed to be 3 rpm (0.314 radian/sec).

In this analysis, the inner part of the refractory layer (3 inches from the inner surface) is replaced by bricks of higher heat capacities and/or thermal conductivities. The rest two-thirds of the refractory layer and the metal shell remain the same. The heat conductivity of existing refractory layer is 1.7 W/m-K (0.982 Btu/hr-ft-^{o}F), and its density and heat capacity are 2,680 kg/m^3 (167.3 lbm/ft^3) and 800 J/kg-K (0.191 Btu/ lbm-^{o}F), respectively. The heat capacity of the high-capacity brick is selected to be 4 times the existing one, which is 3,200 J/Kg-K (0.474 Btu/ lbm-^{o}F). Since the thermal conductivity of the brick usually increases with the heat capacity, a case with the high thermal-conductivity brick is selected to be 4 times the current value, at 6.8 W/m-K (3.928 Btu/hr-ft-^{o}F). Note that these property variations are not targeted to any specific brick materials commercially available. The heat conductivity of the metal sheet is assigned as 16.27 W/m-K (9.40 Btu/hr-ft-^{o}F) and its density and heat

capacity are 8,030 kg/m^3 (501.3 lbm/ft^3) and 502 J/kg-K (0.120 Btu/ lbm-^{o}F), respectively.

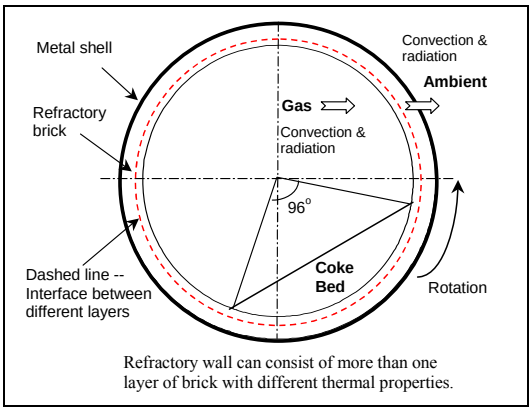

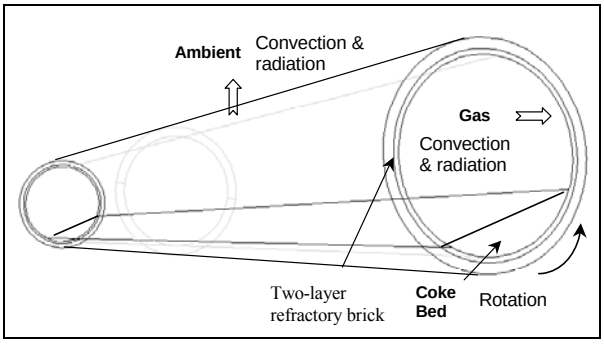

Figure 2 Physical configuration of the kiln. The inner one-third layer is furbished with high heat capacity and/or high-thermal conductivity bricks.

Governing Equations

Since the simulation includes rotational movement, the governing equations must be developed in a rotational frame. Consider a coordinate system which is rotating steadily with an angular velocity $\boldsymbol{\omega}$ relative to a stationary (inertial) reference frame, as illustrated in Fig. 3. The origin of the rotating system is located by a position vector **r**.

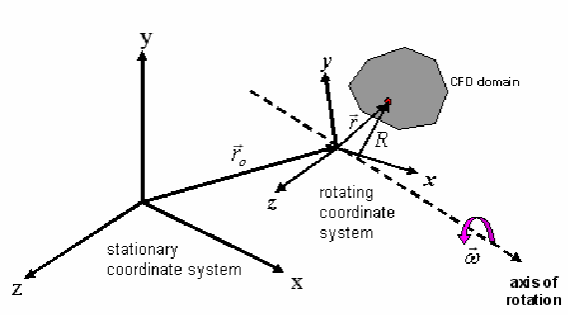

Figure 3 Rotational coordinate for the governing equations [10].

The fluid velocities can be transformed from the stationary frame to the rotating frame using the following relation: $\mathbf{v_r} = \mathbf{v} - \mathbf{u_r}$, Where $u_r = \boldsymbol{\omega} \times \mathbf{r_1}$. In the above, $\mathbf{v_r}$ is the relative velocity (the velocity viewed from the rotating frame), **v** is the absolute velocity (the velocity viewed from the stationary frame), and $\mathbf{u_r}$ is the "whirl" velocity (the velocity due to the moving frame).

The governing equation for an unsteady-state heat transfer is given as

$$\frac{\partial(\rho c_p T)}{\partial t} + \nabla \cdot (\mathbf{v} \rho c_p T) = \nabla \cdot (\lambda \nabla T) + S_h \qquad (1)$$

The source term (S_h) is equal to zero in this study. The velocity field **v** (vector) is computed from the motion specified by the moving reference frames that can be given in this special case as

$$\mathbf{v} = \boldsymbol{\Omega} \times \mathbf{r} \qquad (2)$$

Where $\boldsymbol{\Omega}$ is the angular velocity vector (i.e., the angular velocity of the rotating frame), and **r** is the position vector in the rotating frame.

The thermal boundary condition of the kiln liner wall that encounters combustion gas is modeled as a combined heat transfer mode including both radiation (gas) and convection. Therefore, the total heat transfer is given as

$$q'' = q''_{conv} + q''_{rad} \qquad (3)$$

To consider the radiation heat transfer, the gas temperature, obtained from the 3-D CFD results from Zhang and Wang [11], is set at 1,873 K (or 2,912 ^{o}F) for the long-period study, whereas the gas temperature is input as a function of time for short-period case. An effective wall-gas emissivity is set to 0.15. It is known that the net radiation heat transfer between two gray, diffuse surfaces at T_1 and T_2 is given as

$$q''_{rad} = \sigma(T_1^4 - T_2^4)/(\frac{1-\varepsilon_1}{\varepsilon_1 A_1} + \frac{1}{F_{12} A_1} + \frac{1-\varepsilon_2}{\varepsilon_2 A_2}) \qquad (4)$$

Where ε_1 and ε_2 are the emissivities, and A_1 and A_2 are the areas of Surfaces 1 and 2, respectively. F_{12} is the view factor from Surface 1 to 2. σ is the Stefan-Boltzmann constant, which is equal to 5.67x 10^{-8} W/m^2-K^4 (or 0.1714 x 10^{-8} Btu/hr-ft^2-^{o}R^4). The above equation can be simplified by using an effective emissivity as:

$$q''_{rad} = \varepsilon_{eff} A_1 \sigma(T_1^4 - T_2^4) \qquad (5)$$

The gaseous radiation is related to the concentration of water vapor, carbon oxidizes, coke particles, and the dust in the gas. The gaseous radiation is not a surface phenomenon, but it is instead a volumetric phenomenon and is usually concentrated in specific wavelength intervals (or bands). Following a method developed by Hottel [12], the complicated gas-surface radiation interaction can be simplified by using Equation (4) with

the emissivity obtained from a hemispherical gas mass to a surface. By using the emissivity values of water and carbon dioxide in Hottel [12], the gas emissivity (ε_2) is estimated to be 0.15. The emissivity of the kiln inner wall (ε_1) is estimated to be 0.95. With additional approximations of $A_1 \approx A_2$ and $F_{12} = 1$, the effective emissivity can be found to be 0.15.

The convective heat transfer can be obtained by

$$q''_{cov} = A\ h(T_w - T_{amb}) \qquad (6)$$

Where h is the convective heat transfer coefficient, which can be obtained by calculating the flow velocity and temperature. The convective heat transfer coefficient is assigned as 20 W/m^2K (3.52 $Btu/hr\text{-}ft^2\text{-}^oF$). The reference gas temperature for convection heat transfer is the same as the radiation heat transfer.

Computational Meshes

Global mesh setting The computational domain and the grids are shown in Figs. 4 and 5. For brick layers and metal wall, structured girds are used (1,000 x 26 = 26,000). In the coke bed domain, unstructured grids of 8,000 triangle elements are adopted.

Sliding mesh The sliding mesh scheme is employed to simulate the rotational motion of the metal shell and the brick layers. The coke bed domain is fixed. The rotational speed is set to be 3 rpm.

Buffer Zone

Due to the sliding motion of the geometry, the relative positions between meshes on either side of the moving interface are constantly changing. The gas-brick interface is treated as a boundary, whereas the brick-coke interface is an interior surface. During rotation, the brick surface starts as a boundary when it is in contact with the hot gas, but it changes to an interior interface when the brick is in contact with the coke bed. This brings some challenges to the simulation scheme because mathematically and computationally, an interior surface and a boundary are treated totally differently. To resolve this problem, a thin layer of "buffer zone" (about 5.7% of the brick layer) is created right on top of the brick surface (or inner side of the brick surface) bordering partly with the hot gas and partly with the bottom of the coke bed. This buffer zone is sufficiently thin so that information can be quickly transferred from one side to another side with a negligible impact on the computational results. The buffer zone is stationary. Two layers of mesh are assigned into this buffer zone, and the properties of the buffer zone are assigned the same values as the brick. In this approach, the brick surface will always be treated as an interior interface albeit it is moving. The complication of the original brick boundary surface moving in and out of the computational domain is removed. Now the interfaces between gas and brick and between coke bed and brick are stationary. Designation of the coke surface boundary condition has become convenient and clean.

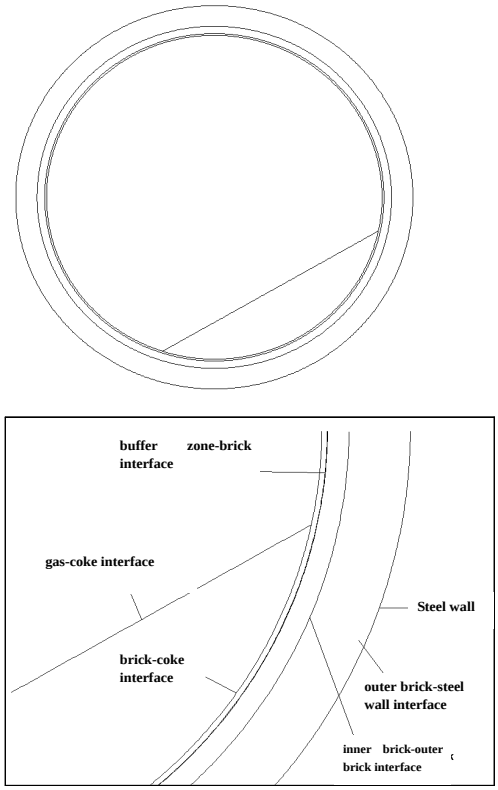

Figure 4 The 2-D cross section geometry and computational interfaces.

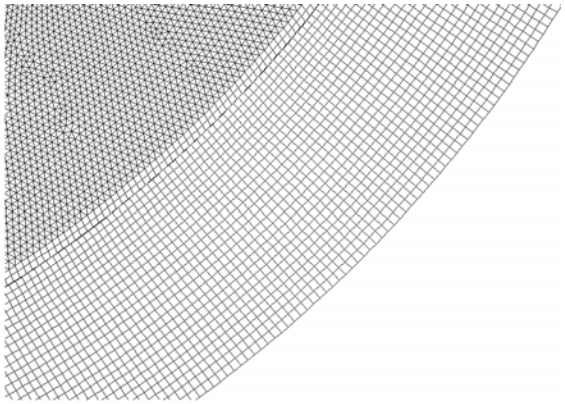

Figure 5 Grid details

Rotational Marching Transient Scheme

The actual kiln is long. The required computational power to conduct a 3-D transient calculation is tremendous, so a simplified approach is made in this study to achieve reasonable results within manageable computational time. In this study, the gas temperature is not calculated, but is adopted from the thorough 3-D

steady-state results performed by Zhang and Wang [11]. The transient conduction is calculated on a 2-D cross section as shown in Fig. 2a. As the calculation proceeds with time, the same cross section is rotating and marching towards next axial location from the feed end to the discharge end, and the local gas temperature will change according to the temperature profile provided by Zhang and Wang (Fig. 6). The total marching time is 45 minutes and is a typical duration for a feedstock moving through the kiln. This rotational marching transient scheme seems works very well; however, the initial temperature condition starting from cold only simulates the situation when the plant restarts after shut down. To provide a more realistic brick wall initial condition for each case, a long-period computation up to 27 hours is conducted first to simulate the situation when the kiln has reached the periodically steady-state condition. The brick temperature distribution resulting from the long-period simulation is used as the initial condition for the 45-minute simulation of a **hot start** with a fresh coke as the new feed. The results of both cold and hot starts are simulated and analyzed.

Initial Conditions

In the real plant-running situations, the petcoke would be discharged after 45~60 minutes of calcining process in the kiln. Two limiting cases are considered first: cold-start and hot-start cases. Considering the operation in the practical situation, except during the cold-start (300K) period, the kiln usually has been continuously running for weeks and months when the raw petcoke is fed into the kiln. Under this condition, the temperature inside the brick layer is nearly periodically steady with some minor temperature fluctuations. In other words, the brick is usually already hot and reached the periodically steady state for most feeding condition. Therefore, the steady-state temperature (1740K- 1600K) within the bricks is used as the initial condition for the hot-start cases. In this approach, the hot-start initial condition will be an upper limiting case for the real condition. The steady-state case is the result of running the transient case to 27 hours with a completely cold start. The actual initial brick temperature should be lower than the steady state temperature because before it reaches steady state, the petcoke has already been discharged which takes about 45~60 minutes, whereas the steady state needs about 27 hours to reach from the cold start. Therefore a third initial condition with the brick temperature uniformly assigned at 1200K is selected to represent a case more close to the actual initial brick temperature.

Boundary Conditions

The hot gas temperature distribution inside the kiln is not uniform and is expected to have a strong effect on the heat transfer behavior inside the bricks. In order to simulate the effect of the changing gas temperature inside the kiln, the 3-D CFD results from Zhang and Wang [11] as shown in Fig. 6 is input via user defined function (UDF) as a function of time to Fluent. The temperature distribution in Fig. 6 represents the centerline temperature along the axial length of the kiln. Since we use the rotational transient marching scheme, the actual axial location can be converted to the time-domain for each specific rotational speed (RPM). Figure 6 shows the temperature distribution of the inside hot air with respect to the time that coke stays in the kiln instead of length as originally shown in Zhang and Wang's report. Table 1 summarizes the inlet and boundary conditions on different surfaces.

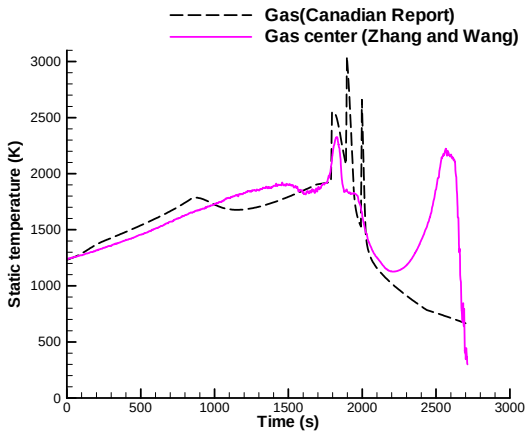

Figure 6 Centerline gas temperature distributions in the kiln from the 3-D DFD results from [4]. The Canadian report is from [15]. The spatial coordinate (distance from the kiln feed end) is transformed to the temporary coordinate (time after petcok is fed in the kiln) for 3 rpm.

TABLE 1 Summary of inlet and boundary conditions

Surfaces	BC type	Values	
Hot gas - brick	Radiation +Convection	Gas temperature for radiation and convection	Varying (Fig. 6)
		Effective wall-gas emissivity	0.15
		Heat transfer coefficient	20 W/m^{2}K (3.52 Btu/hr-ft^2-^{o}F)
Hot gas - coke	Radiation +Convection	Gas temperature for radiation and convection	Varying (Fig. 6)
		Effective wall-coke bed emissivity	0.15
		Effective heat transfer coefficient	100 W/m^{2}K (17.6 Btu/hr-ft^2-^{o}F)
Outer surface (ambient)	Radiation +Convection	Effective radiation temperature	200 K (-99.6^{o}F)
		Emissivity	0.85
		Convection reference temperature	300 K (80^{o}F)
		Heat transfer coefficient	10 W/m^{2}K (1.76Btu/hr-ft^2-^{o}F)

The boundary condition of the outer surface is also modeled as a combined mode of radiation and convection. The emissivity of the outer metal surface is assumed to be 0.85. The ambient radiation temperature is difficult to decide. For the lower half of the kiln, the radiation occurs between the kiln surface and surrounding objects. The reference radiation temperature should be close to the ambient temperature. For the upper half of the kiln, the radiation goes to the sky. A radiation temperature much

lower than the ambient temperature is possible when the sky is clear or transparent. Considering these factors as well as the average effect due to kiln's rotation, the effective temperature for the radiation is set to 200K (-99.67 ^{o}F). The model of the convective heat transfer considers both the natural and forced convections. With a wind speed of 5 mile/hr and a surface temperature of 600 ^{o}F, the convective heat transfer coefficient is set to 10 W/m^{2}K (1.76 Btu/hr-ft^2- ^{o}F). The detailed calculation is documented in [13]. The convective reference temperature is set to the ambient temperature 300K (or 80 ^{o}F). The inlet condition is assigned based on the actual feeding condition at 300 K.

The most complicated condition occurs at the coke bed. The coke bed is a dynamic granular flow; the heat transfer between the coke and the air is modeled as a combined mode of radiation and convection via the granular contacts between the porous coke bed and the air. Considering the tumbling and the granular motion of the coke bed, an **effective thermal conductivity** is assigned inside the coke bed with a value 10 times of the thermal conductivity of the solid petcoke and an effective heat transfer coefficient (five times higher) is assigned over the gas-coke interface as shown in Table 1. Similar to the gas-brick interface, an effective gas-coke bed emissivity of 0.15 is assigned.

Sign convention: It needs to be noted that the heat flux is assigned positive when heat flows in the direction of the radius direction (from inside the kiln to outside). The integrals of heat flux on different faces apply the same sign convention.

Simulated Cases

Total four cases and 9 subcases have been simulated and their property values are shown in Table 2:

- **Case 1 (Cp, k, steady state) -** achieve the periodically steady-state condition by computing 27 hours of operation starting from cold with existing Cp and k values.
- **Case 2 (Cp, k, 45 minutes) -** With the existing brick properties, starting at cold (Case 2C), hot (Case 2H), and uniformly at 1200K.
- **Case 3 (various Cp, k values, steady state) -** achieve the periodically steady-state condition by computing 27 hours of operation starting from cold with a combination of (4Cp, k), (Cp, 4k) and (4Cp, 4k) subcases.
- **Case 4 (4Cp, 4k, 45 minutes) -** Bricks with both four times higher heat capacity and thermal conductivity, starting at cold (Case 4C), hot (Case 4H), and uniformly at 1200K.

Table 2 Brick properties for various cases

Case No.	Coke k , W/m-K (Btu/h-ft-^{o}F)	Brick Cp, J/kg-K (Btu/lbm-^{o}F)	Brick k, W/m-K (Btu/h-ft-^{o}F)
Cases 1, 2	17.3 (9.99)	800 (191,080)	1.7 (0.982)
Case 4	17.3 (9.99)	3200 (764,320)	6.8 (3.929)

RESULTS AND DISCUSSION

Steady-State Case 1

The steady-state case is computed first up to 27 hours of real-time operation with the kiln rotating at 3 rpm. As explained before, the result of the steady-state case will be used as the initial condition for the hot-start cases. In the meantime, observation of the long-period development of the temperature and heat flux in the kiln provides the insight to the major features of the heat transfer dynamics among hot gas, brick wall, and coke bed. The results are not shown but are summarized below:

1. Effect of long-period marching time (Case 1)
   - Temperatures of both the brick and the coke bed increase with time due to the heat transferred from the hot gas. Theoretically, the temperature distribution will reach the periodically steady-state condition as time goes to infinity. **Periodically steady state** means the temperature of a specific brick experiences a cyclic temperature changes with repetitive values.
   - Heat flux at the gas-brick interface decreases with time, because as the brick temperature goes up, temperature difference between the hot gas and brick decreases.
   - The changing trend of heat flux at the gas-coke bed interface is similar to that at the gas-brick interface.
   - On the interface between coke bottom and brick, heat flux increases first with time, and then decreases. Since the radically outward heat flux is defined as "positive," this result implies that the brick does store thermal energy during the period when it is in contact with the hot gas but releases the energy to the coke bed when it is in contact with the coke bed in early part of the process. Eventually the coke bed will become hotter than the brick and reverse heat transfer from the coke bed to the brick.
2. Effect of a higher brick Cp value (Case 3 with 4Cp, k)
   - High Cp renders lower brick temperature, which increases heat flux from gas to brick, but decreases heat flux from brick to coke bed. Lower brick temperature provides a lager temperature gradient between the hot gas and the brick layer, so the heat flow from gas to the brick layer increases. However, lower brick temperature reduces the temperature gradient between the brick layer and the coke bed

resulting in reduced heat flux.

- Higher Cp value requires longer time to reach periodically steady-state condition. The effect of Cp value diminishes with time.
- In consistency with the postulation**,** increasing brick's Cp value does help brick absorb more heat from the hot gas. However, in contrast to the postulation, heat transfer from the brick to the coke bed is reduced.

3. Effect of higher brick k value (Case 3 with Cp, 4k)
   - It takes longer to reach steady state with a higher k value, which is favorable to our motivation because heat goes constantly at higher rate from brick into coke.
   - Increasing k-value gives more pronounced influence on heat transfer than increasing Cp-value.

Starting with cold brick for 45 minutes (cold-start):

The results of the cold-start cases are shown in Figs. 7 and 9 for temperatures and heat flux distributions on gas-coke interface and the inner brick surface, respectively. Figures 8 and 10 show the integral results of heat flux over several surfaces including brick-coke interface, gas-coke interface, outside steel wall surface, etc. Together with these results, the total heat flow entering into the coke layer is calculated and compared with the heat that is transferred from the brick into the coke bed. These two cold-start cases are designated as Case 2C and Case 4C. Comparisons of these two cases (Figs. 7-10) are summarized below:

1. Temperature variations with time on gas-brick interface and gas-coke interface are mostly following the change of the hot gas temperature variation with a short time delay.
2. Temperatures in the brick and coke bed continuously increase with time during the 45-minute calcining process.
3. Heat flows from hot gas into both brick layer and coke bed increase in the first 25 minutes (1500 seconds) but decrease afterwards due to increased coke and brick temperatures which result to reduced gas-coke and gas-brick temperature gradients.
4. The brick layer does store thermal energy from hot gas and transport it to the coke bed. Increasing k and Cp values in Case 4C adversely affects this energy transport to a negligible level (Fig. 10) due to reduced brick temperature. This is similar to the conclusions derived from the long-period steady-state results.
5. Heat loss through the outside wall is relatively small, so the results presented here should be valid for the situation when the k of outer layer brick is reduced to compensate for the increased k in the inner brick layer.

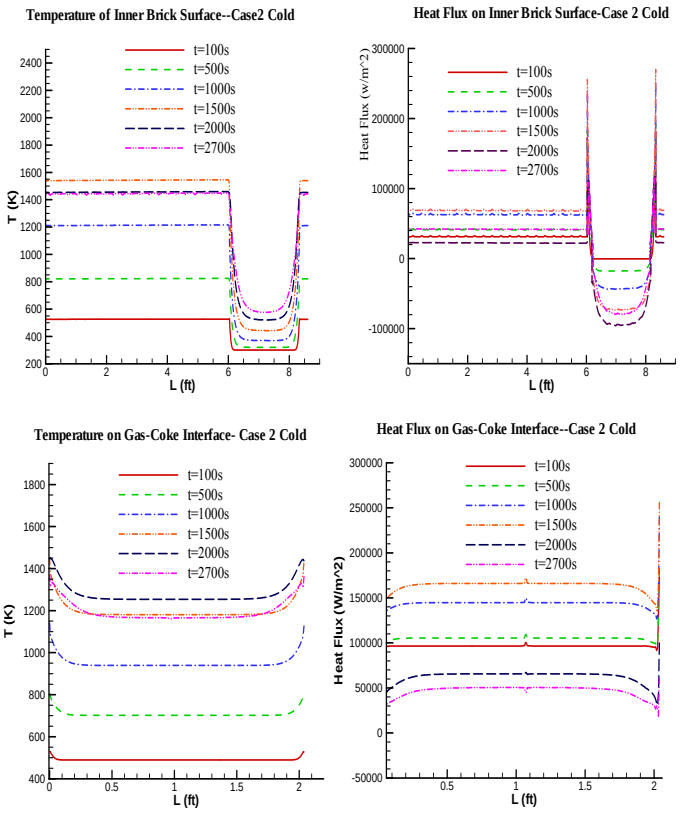

Figure 7 Temperature and heat flux distributions of Case 2C, starting cold.

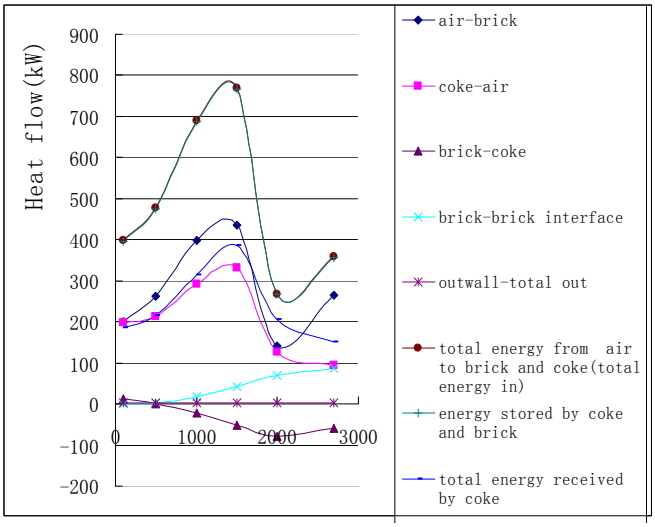

Figure 8 Integral of heat flux over various interfaces of Case 2C, starting cold

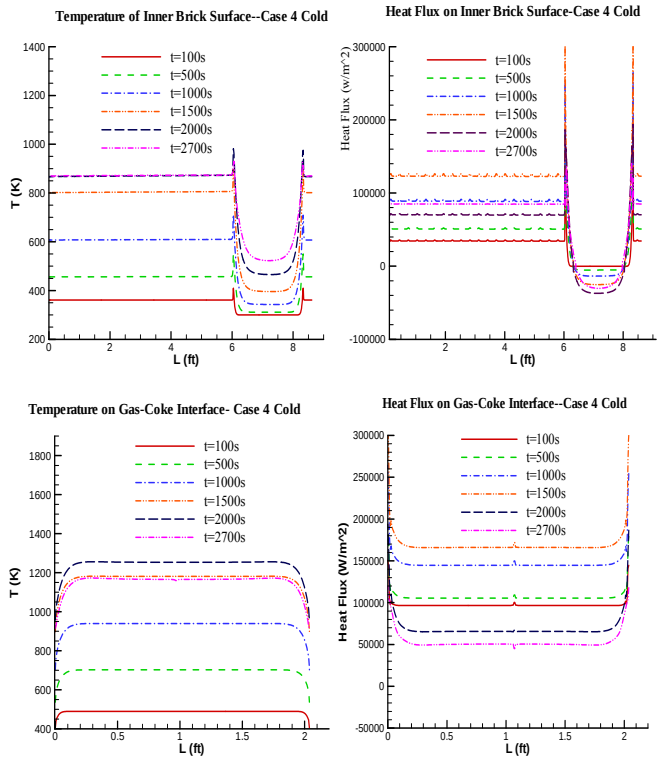

Figure 9 Temperatures and heat flux distributions of Case 4C, starting cold

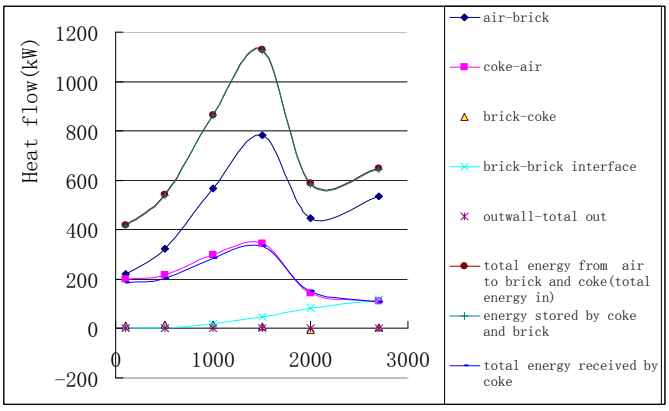

Figure 10 Integrate heat flux over various interfaces of Case 4C, starting cold

Starting with hot brick for 45 minutes (hot-start):

Cases 2 and 4 with hot-start conditions are designated as Cases 2H and 4H, respectively. Temperature and heat flux distributions on gas-coke interface and inner brick surface are shown in Figs. 11 and 13 for Cases 2H and 4H, respectively. Figures 12 and 14 show the integral results of heat fluxes over various interfaces. Comparison of Cases 2H, 4H, 2C and 4C are summarized below:

1. Figures 12 and 14 show that temperature and heat flux inside the brick layer do not have much difference between Cases 2H and 4H. This is reasonable because long-period brick layer temperatures are used as the initial conditions.
2. Temperature variations with time on gas-brick interface and gas-coke interface follow the change of gas temperature, irrespective of the initial conditions (hot or cold start) or the property variations (high or low k and Cp values).
3. Temperatures inside both brick and coke continuously increase with time. Hot start limits the temperature increase in the brick layer within 200K, but the temperature increase trend in the coke bed does not change too much between the cold and hot starts because the petcoke is fed fresh entering the kiln at ambient temperature for all cases.
4. Hot start favorably increases the brick's function in transporting energy from the gas to the bottom of coke bed. The integral results shown in both Cases 2H (Fig. 12) and Case 4H (Fig. 14) indicate appreciable amounts of energy from 100 to 600 kW is transported by the brick layer at each instant of time (or at each cross section of the kiln). The integral energy curve of Case 4H in Fig. 14 is less responsive to the temperature change in the hot gas than the curve of Case 2H in Fig.12 due to increased k and Cp values. **The advantage of Case 4H over Case 2H is not discernable.**
5. The initial brick temperature for hot-start cases is near 1700 K, which clearly overestimates the initial brick temperature (or temperature at the feeding end). Therefore, the appreciable energy transferred from the brick to coke bed is believed to be overestimated.
6. Heat loss through the outside wall is relatively small in all cases, so the results presented here should be valid for the situation when the k of outer layer brick is reduced to compensate for the increased k in the inner brick layer.

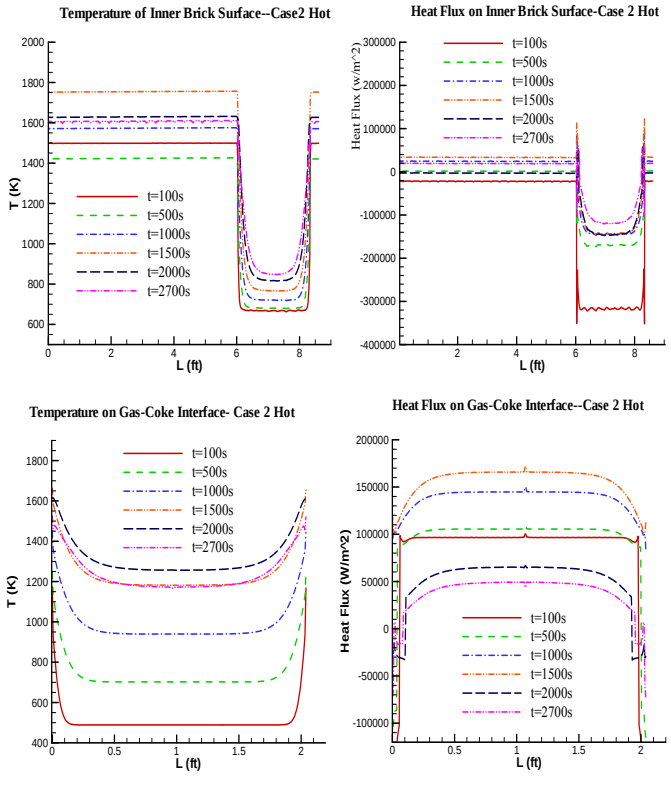

Figure 11 Temperatures and heat flux distribution of Case 2H, starting hot.

Figure 13 Temperatures and heat flux distribution of Case 4H, starting hot.

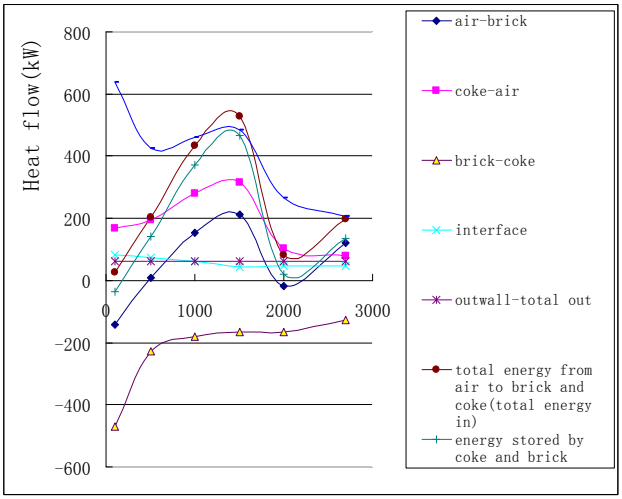

Figure 12 Integral heat flux over various interfaces of Case 2H, starting hot.

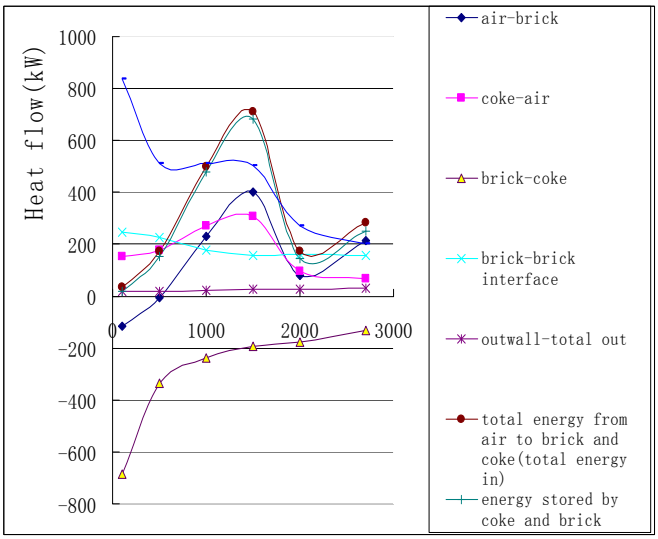

Figure 14 Integral heat flux over various interfaces of Case 4H, starting hot.

Starting with 1200K brick temperature for 45 minutes:

Between cold and hot start cases, uniform brick temperature at 1200K for Cases 2 and 4 are studied. Temperature and heat flux distributions on gas-coke interface and inner brick surface are shown in Figs. 15 and 17 for Cases 2 and 4, respectively. Figures 17 and 19 show the integral results of heat fluxes over various interfaces including brick-coke interface, gas-coke interface, outside steel wall surface, etc. Comparison of Cases 2H, 4H, 2C, 4C and 1200k start are summarized below:

1. Comparing Case 2 and Case 4 with 1200k start, Case 4 (4Cp, 4k) renders lower brick temperature, which increases heat flux from gas to brick, but decreases heat flux from brick to coke bed. Lower brick temperature provides a lager temperature gradient between the hot gas and the brick layer, so the heat flow from gas to the brick layer increases. However, lower brick temperature reduces the temperature gradient between the brick layer.
2. For 1200K start, heat flux from brick to coke bed is about the same between Case 2 and Case 4. Case 2 is slightly higher than Case 4 (< 5%). This is because although Case 4 has bigger k compared with Case 2, smaller temperature gradient counters its effect and thus making the heat flux from brick to coke about the same between the two cases.
3. For 1200k starting both cases, heat flux from brick to coke bed is much less than the hot start cases.

In summary, the hot-start cases overestimate the heat transferred from the brick to the coke bed, while the cold-start cases underestimate the brick-coke heat transfer. The actual case should be a bit better than the cold-start cases. Appreciable heat (100-600kW) is transported from the brick to the coke bed for one rotation for both lower and higher Cp and k bricks. The advantage of using bricks of higher Cp and k are not significant.

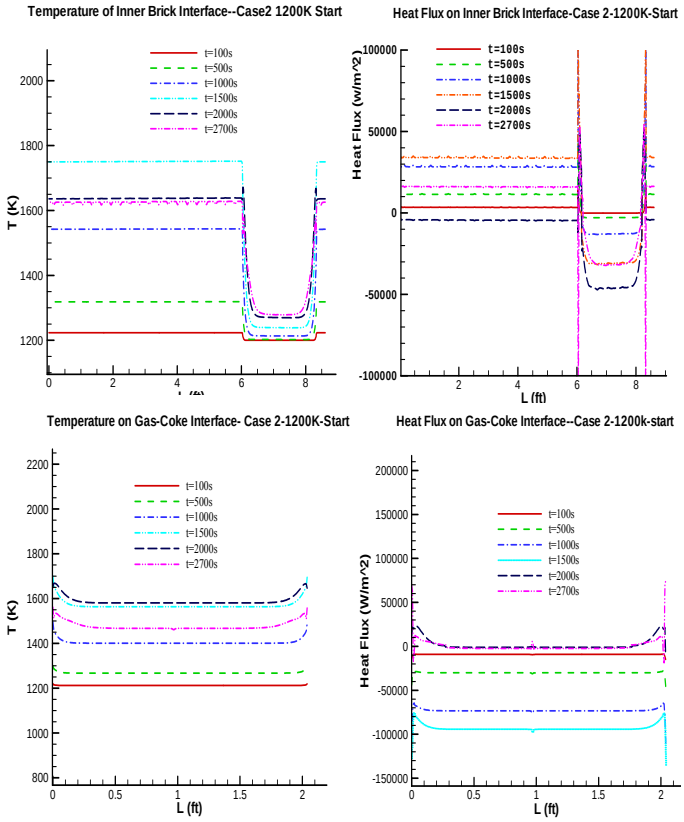

Figure 15 Temperatures and heat flux distribution of Case 2, 1200k start.

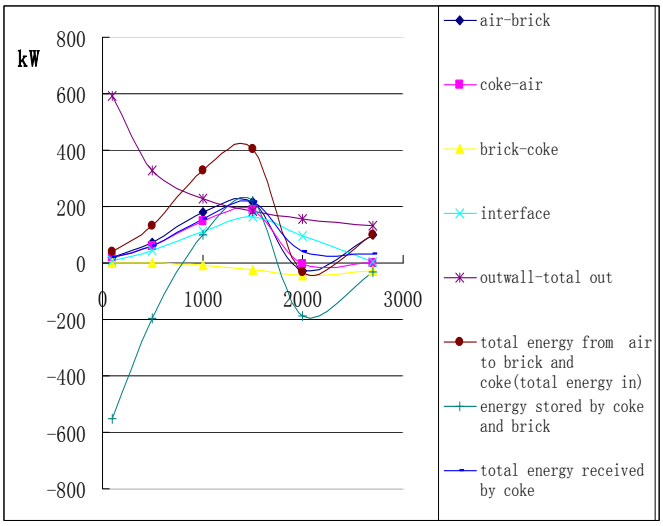

Figure 16 Integral heat flux over various interfaces of Case 2, 1200k start.

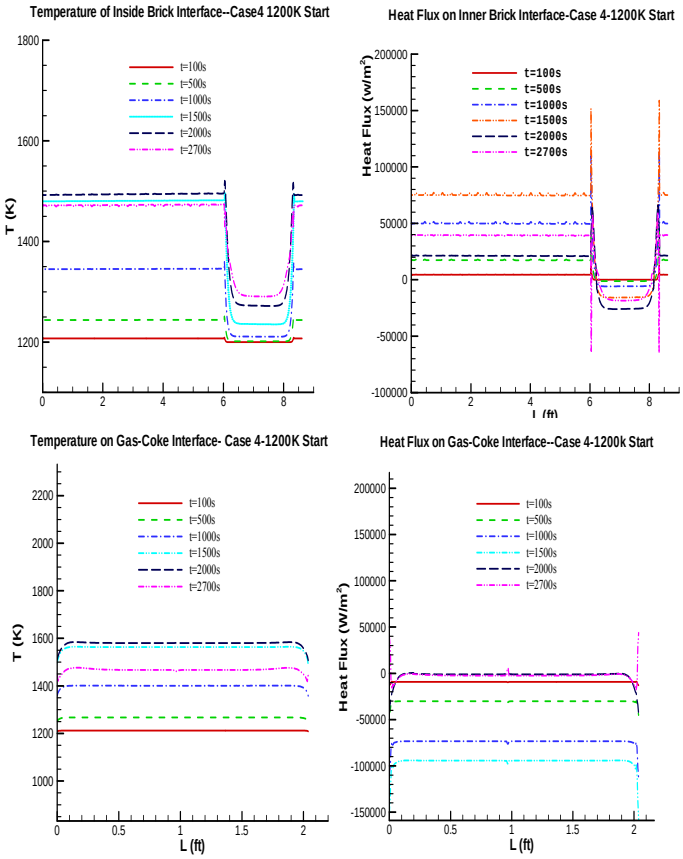

Figure 17 Temperatures and heat flux distribution of Case 4, 1200k start.

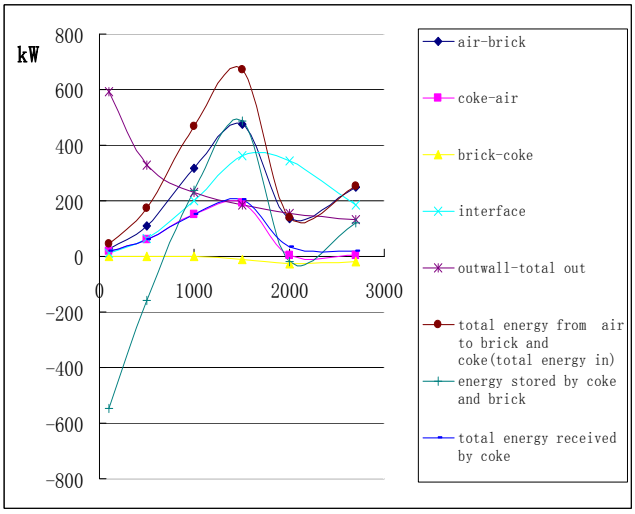

Figure 18 Integral heat flux over various interfaces of Case 4, 1200k start.

CONCLUSIONS

This study investigates the potential energy saving benefit by replacing inner one third of the current brick layer with higher heat capacity and/or higher thermal conductivity bricks. Numerical simulations are conducted and analyzed by using the rotational transient marching scheme which converts a 2-D rotational transient domain to an equivalent 3-D steady-state rotational domain. The conclusions are:

- Increasing the heat capacity of the brick layer reduces brick temperature and helps increase the heat transfer between the hot gas and the brick; in other words, it does help brick store more heat from the hot gas, but heat transfer between the brick and the coke is reduced, which is opposite to the original postulation.
- Higher brick thermal conductivity decreases brick temperature thus increases heat transfer between hot gas and the brick layer. The heat transfer from the brick to the coke bed is also increased but not significantly
- Usually a brick with a higher Cp value also has a higher k-value. Simulations of a brick layer with both four times higher Cp and k values actually show a reduction of the brick temperature, and hence, a degradation of the heat-transfer between the brick and coke. Therefore, replacing the existing brick layer with a high Cp and/or high k value brick is not recommended.
- The heat lost from the outer surface is relatively small irrespectively of the change of property of the inner brick layer.

ACKNOWLEDGEMENTS

This study was supported by CII Carbon, LLC. Part of the funding was provided by the Louisiana Board of Regents' Industrial Ties Research Subprogram.

REFERENCES

[1] Ellis, P. J., and Paul, C. A., 2000, "Tutorial: Petroleum Coke Calcining and Uses of Calcined Petroleum Coke," AIChE 2000 Spring National Meeting, Third International Conference on Refining Processes, Session T9005.

[2] Bagdoyan, E. A., and Gootzait, E., 1985, "Refiners Calcine Coke," Hydrocarbon Processing, pp.85-90.

[3] Buir, T., Perron R, 1993, "Model-Based Optimization of The Operation of the Coke Calcining Kiln," Carbon (Carbon), 31, pp. 1139-1147.

[4] Dhanjal, S. and Barr, P., 2004, "The Rotary Kiln: An Investigation of Bed Heat Transfer in the Transverse Plane," Metallurgical and Materials Transactions B, 35, pp. 1059-1070.

[5] Jochen, M., Eckehard, S., Xiaoyan L., 2004, "Prediction of Rolling Bed Motion in Rotating Cylinders," AIChE Journal, 50, pp. 2783-2793.

[6] Gorog, J. P., Brimacombe, J. K. and Adams T. N., 1981, “Radiative Heat Transfer in Rotary Kilns,” Metallurgical and Materials Transactions B, 12, pp. 55-70.

[7] John, R. F., Dilip, K. S., 1991, “Rotary Kiln Transport Processes,” AIChE Journal, 37, pp 747-758.

[8] Perron, R., Buir, T., 1990, “Rotary Cylinders: Solid Transport Prediction by Dimensional and Rheological Analysis,” Canadian. J. Chem. Eng, 68, pp. 61-68.

[9] Henein, H. and Brimacombe, J. K. and Watkinson, A. P., 1983, “The Modeling of Transverse Solids Motion in Rotary Kilns,” Metallurgical and Materials Transactions B, 14, pp 207-220.

[10] Fluent 6.3 User’s Guide, September 2006, Fluent Inc.

[11] Zhang, Z. and Wang, T., 2007," Thermal-Flow and Combustion Simulation in a Rotational Calcining Kiln," ECCC Report 2007-02, Energy Conversion and Conservation Center, University of New Orleans, submitted to CII Carbon, LLC.

[12] Hottel, H. C., 1954, *Radiant-Heat Transmission*, in W. H. McAdams, Ed., Heat Transmission, 3rd. ed., McGraw-Hill, New York.

[13] Wang, T. and Li, X., 2006, “Evaluation of Potential Benefits Using Higher Thermal Conductivity Bricks in a Calcining Kiln,” ECCC Report 2006-01, Energy Conversion and Conservation Center, University of New Orleans, submitted to CII Carbon, LLC.

[14] Li, X. and Wang, T., 2005, “Analysis of Energy Savings by Painting the Calcining Kiln Surface,” ECCC Report 2005-06, Energy Conversion and Conservation Center, University of New Orleans, submitted to CII Carbon, LLC, June.

[15] CII Rotary Coke Calciner Modeling-1D Coke Calcination, Vol. 2, 2004.